

Research report

Functional analysis of glutamate transporters in excitatory synaptic transmission of GLAST1 and GLAST1/EAAC1 deficient mice

Wilhelm Stoffel^{a,*}, Rafael Körner^a, Dagmar Wachtmann^b, Bernhard U. Keller^b

^aLaboratory of Molecular Neuroscience, Faculty of Medicine, Center of Molecular Medicine Cologne (CMMC), Institute of Biochemistry, University of Cologne, Joseph-Stelzmannstraße 52, D-50931 Köln, Germany

^bZentrum Physiologie und Pathophysiologie, Humboldtallee 23, 37337 Göttingen, Germany

Accepted 14 June 2004

Available online 29 July 2004

Abstract

The high affinity, Na⁺-dependent, electrogenic glial L-glutamate transporters GLAST1 and GLT1, and two neuronal EAAC1 and EAAT4, regulate the neurotransmitter concentration in excitatory synapses of the central nervous system. We dissected the function of the individual transporters in the monogenic null allelic mouse lines, *glast1*^{-/-} and *eaac1*^{-/-}, and the derived double mutant *glast1*^{-/-}*eaac1*^{-/-}. Unexpectedly, the biochemical analysis and the behavioral phenotypes of these null allelic mouse lines were inconspicuous. Inhibition studies of the Na⁺-dependent glutamate transport by plasma membrane vesicles and by isolated astrocytes of wt and *glast1*^{-/-} mouse brains indicated the pivotal compensatory role of GLT1 in the absence particularly of GLAST1 and GLAST1 and EAAC1 mutant mice. In electrophysiological studies, the decay rate of excitatory postsynaptic currents (EPSCs) of Purkinje cells (PC) after selective activation of parallel and climbing fibers proved to be similar in wt and *eaac1*^{-/-}, but was significantly prolonged in *glast1*^{-/-} PCs. Bath application of the glutamate uptake blocker SYM2081 prolonged EPSC decay profiles in both wt and double mutant *glast1*^{-/-}*eaac1*^{-/-} PCs by 286% and 229%, respectively, indicating a prominent role of compensatory glutamate transport in shaping *glast1*^{-/-}*eaac1*^{-/-} EPSCs.

© 2004 Elsevier B.V. All rights reserved.

Theme: Neurotransmitters, modulators, transporters, and receptors

Topic: Uptake and transporters

Keywords: Excitatory synapse; Glutamate transporters; Transporter null mouse mutants; EPSC profiling

1. Introduction

Neurotransmission in excitatory, glutamatergic synapses of CNS is regulated by the concentration of the major neurotransmitter L-glutamate, the activity of the glutamate receptors, at the postsynaptic membrane and high affinity neurotransmitter transporters bordering the synaptic cleft. Glutamate transporters are believed to play an important role in synaptic plasticity [6,8] and development [13,35,37]. Persisting high synaptic L-glutamate concentrations trigger

neuronal death [14]. Neurotoxic concentrations of glutamate in the synaptic cleft may occur in cells during cerebral hypoxia due to the lack of energy for maintaining the electrochemical membrane potential followed by a reversed glutamate transport [50]. Impaired L-glutamate transport has been discussed as primary or secondary cause of neurodegenerative diseases, e.g. special forms of amyotrophic lateral sclerosis [7,43], Huntington disease [40] and Alzheimer's disease [44].

A family of five structurally related Na⁺-dependent L-glutamate transporters, GLAST1 (EAAT-1) [49], GLT-1 (EAAT-2) [42], EAAC1 (EAAT-3) [25], EAAT-4 [22] and EAAT-5 [4] has been described. Their homologies and strikingly similar hydrophobicity pattern indicate a comparable membrane topology.

* Corresponding author. Tel.: +49 221 478 6881; fax: +49 221 478 6882.

E-mail address: wilhelm.stoffel@uni-koeln.de (W. Stoffel).

GLAST1 (EAAT1) [49], and similarly GLT-1 [30,31,42] are mainly expressed in astrocytes, e.g. Bergmann glia cells of cerebellum, in the hippocampus and throughout the cortex. EAAC1 (EAAT-3) is not only strongly expressed in peripheral tissues (kidney, gut) but is also found in the CA2 to CA4 regions of the hippocampus, the dentate gyrus, the granular layer of the cerebellum, and the cerebral cortical layers (II to IV) [25,39]. EAAT-4 expression restricted to cerebellar Purkinje synapses [17] and similarly EAAT5, mainly expressed in retina, are glutamate transporters with additional ligand gated chloride channel activity [4].

We studied the function of the three dominant glutamate transporters individually, of GLAST1 and EAAC1 in vivo in the two monogenic null allelic *glast1*^{-/-}, *eaac1*^{-/-} mouse lines and of GLT-1 in the derived double mutant *glast1*^{-/-}*eaac1*^{-/-}. The mouse GLAST1 gene was disrupted by homologous recombination in mouse embryonic stem cells (ES) similar to the generation of the *eaac1*^{-/-} mouse [41]. Crossing the *glast1* locus into the *eaac1*^{-/-} background yielded the double “knock out” *glast1*^{-/-}*eaac1*^{-/-} mutant with a complete GLAST1 and EAAC1 deficiency. Unexpectedly, the phenotype of the three homozygous mutants is inconspicuous. Neither neurodegeneration nor behavioral abnormalities were observed. The *glast1*^{-/-} mouse mutant was also generated earlier with a different gene-targeting construct [54]. Unlike our *Glast1*-deficient mutant and the *glast1*^{-/-}/*eaac1*^{-/-} double mutant reported here, this mutant showed impaired motor coordination but only at a high speed rotarod challenge.

Cerebellar Purkinje cells (PCs) are a prominent model system to evaluate neurotransmitter profiles at the synapse. Whole cell recording of the long-lasting AMPA EPSCs displayed by glutamatergic synapses of Purkinje cells induced by the selective activation of climbing and parallel fibers in cerebellar slices of the three null mutant mice, associated with transporter inhibition studies unveiled the dominant role of GLT1 over GLAST1 and the negligible contribution of EAAC1, data, which are also supported by glutamate uptake studies in vitro with plasma membrane vesicles and the biochemical analysis.

2. Materials and methods

2.1. Characterization of the mouse GLAST1 gene and construction of replacement vector

GLAST1 genomic sequences were isolated from a λ EMBL-3 129 mouse leukocyte genomic library (Clontech ML1040j) with a genomic hGLAST1 probe [48]. Fig. 1A resembles the exon–intron organization of the 5' region of the GLAST1 gene with exons I and II used to construct the replacement vector for homologous recombination in which exon II is replaced by the neomycin resistance gene (*neo*). A 1.7-kb *Bam*HI/*Nde*I fragment was ligated blunt ended into

the *Xho*I restriction site of the pPNT vector. The *Nde*I fragment with exon I was replaced by the *pgk* neo gene (Fig. 1A). The *Nde*I/*Spe*I fragment was inserted into the *Xba*I restriction site of the first ligation step downstream of *pgk-neo*. The replacement vector was linearized at the *Cla*I restriction site (Fig. 1A). The negative selection marker, the thymidin kinase (*pgk-tk*) gene was inserted at the 3' end of the targeting genomic sequence.

2.2. Homologous recombination in mouse ES cells

R1 embryonic stem (ES) cells were transfected with 20 μ g of the linearized targeting vector, positive ES cell clones selected and their DNA genotyped by Southern blot hybridization following established procedures, *Nco*I digested and analyzed by Southern blot hybridization. A P³²-labeled 350-bp *Hind*III/*Sac*I fragment, the 5' flanking region of the λ clone outside the insert sequence, was used as hybridization probe. The homologous recombination event was verified by *Hind*III digestion which yielded a 6.3-kb fragment in case of homologous recombination and a 4.8-kb fragment from the *wt* allele. ES cell clones were injected into CD1 blastocysts to produce germline chimeric male [9], which were crossbred to homozygosity. *Bam*HI restriction of the homozygous double mutant *glast1*^{-/-}*eaac1*^{-/-} revealed the RFLP expected from the single mutant *eaac1*^{-/-} [41].

2.3. RNA analysis

RNA was isolated from total brain [15] and separated on a denaturing formaldehyde agarose gel (1.2%) electrophoresis. A *Hind*III/*Eco*RI fragment containing exon II of GLAST1 and cDNA probes of EAAC1 and GLT-1 were used for Northern blot hybridization analysis. A GAPDH cDNA fragment served as internal control.

2.4. Western blot hybridization analysis

Mouse brain was homogenized in 1 ml lysis buffer (100 mM Tris/HCl pH 8.0; 0.1% 2-mercaptoethanol; 10% glycerin, 1% Triton X-100) and centrifuged for 15 min at 14,000 \times g and 4 °C. Three protein aliquots of the supernatant (20, 40 and 60 μ g) were separated by SDS-PAGE (12%) and then electroblotted to a nitrocellulose membrane (Schleicher and Schüll). The membrane was blocked with 3% bovine serum albumin (BSA). The blot was treated sequentially with affinity-purified polyclonal anti GLAST1 (1:3000) and anti-rabbit alkaline phosphatase conjugated second antibody. The band intensities were digitalized and quantified using the SCION Image software of the phosphoimager. The intensities of the EAAT4 band were similar in *wt* and *glast1*^{-/-} mice, whereas the intensities of the GLT1 bands of the *wt* aliquots exceeded the intensity of the *glast1*^{-/-} mice by a factor of 2 to 3 (2.2, 2.7, 2.1 for the 20, 40, 60 μ g protein aliquots, respectively).

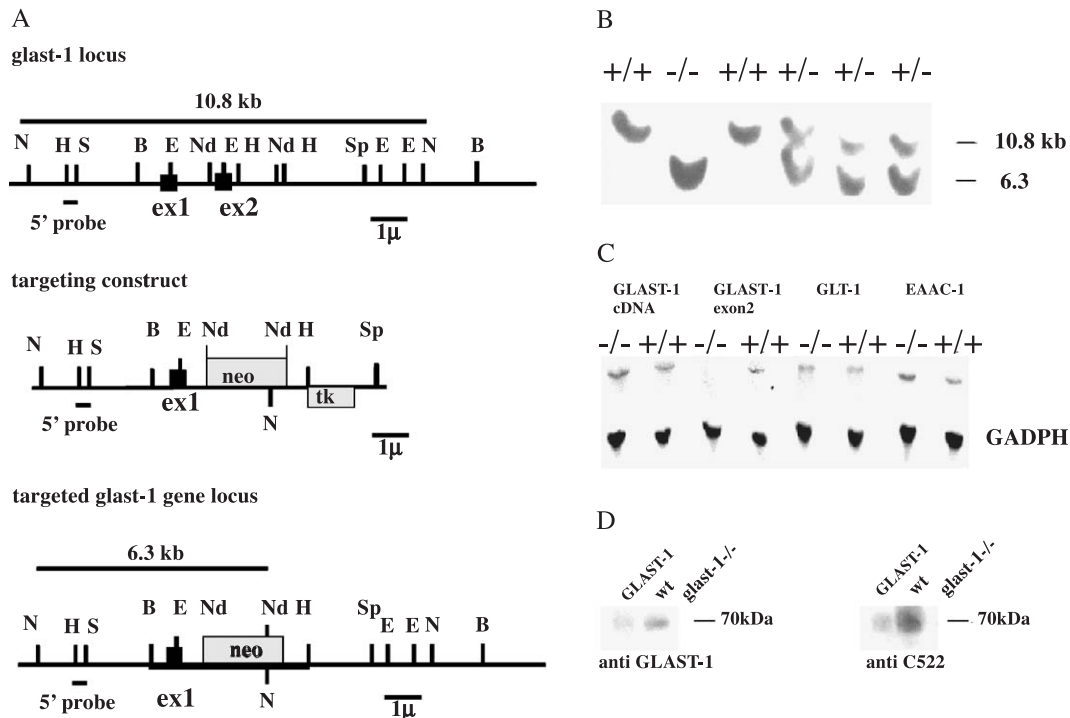


Fig. 1. Targeted disruption of the *GLAST1*-gene. (A) Schematic presentation of the *wt* *GLAST1* locus, the targeting vector and the targeted *GLAST1* locus. Exon: closed boxes. Targeted allele: exon II is replaced by the *neo* gene of the pPNT vector. *Hind*III restriction of the genomic DNA releases a 4.8-kb fragment diagnostic for the *wt* locus and a 6.3-kb fragment for the *glast1* locus detected with the 5' external probe, indicated by the bar. The diagnostic *Bam*HI RFLP for the *eaac1*^{-/-} locus has been reported before. (B) Southern blot analysis of tail DNA of F2 littermates. -/- homozygotes; +/- heterozygotes, +/+ wild type. (C) Northern blot hybridization analysis of brain RNA. The transcripts of the *GLAST1* gene are lacking exon II as indicated by the missing signal in (D) when exon II probe is used for hybridization. (D) Western blot analysis of solubilized membrane proteins of total brain separated by SDS-PAGE (10%). Positive control: purified *GLAST1* protein. The affinity purified anti-*GLAST1* antibody and likewise anti-C522 (kindly provided by Dr. Danbolt) recognizes the 66-kDa *GLAST1* protein in *wt* but not in *glast1*^{-/-} mutant mice.

2.5. Vesicular glutamate uptake assay

The vesicular glutamate uptake was assayed *in vitro* [45]. Cerebella of 6–8-month-old mice were used for the membrane preparation. Aliquots of the membrane suspension (100 μg protein) were suspended in 100 μl ECS buffer (150 mM NaCl, 3 mM KCl, 1 mM MgCl₂, 1 mM CaCl₂, 10 mM HEPES, 10 mM glucose, pH 7.4) containing 0.05 μCi (110,000 dpm) [¹⁴C]-glutamate (250 mCi/mmol) and 10 μM glutamate. Duplicate assays were performed in ECS buffer, ECS buffer in which Na⁺ was substituted by choline chloride, and ECS buffer supplemented with 0.01–1 mM DL-threo-hydroxyaspartate (THA) or with 0.5–1 mM dihydrokainate (DHKA). The assay mixtures were incubated for 4 min at 37 °C. Transport was terminated with 200 μl ice-cold Na⁺-free ECS buffer. The assay mixture was centrifuged for 2 min at 14,000×g and 4 °C, the pellet washed three times with Na⁺-free ECS and dissolved in Bray's solution for counting of the radioactivity.

2.6. [¹⁴C]-L-glutamate uptake by astrocytes in cultures

Astrocytes from 2-day-old *wt* and *glast1*^{-/-} mouse brains and isolated cerebellae were isolated and cultured for up to 5

weeks following established protocols adapted to mouse tissue [36]. Cells were grown in Petri dishes for at least 2 days and preincubated with ECS for 30 min, followed by the addition of [¹⁴C] glutamate (0.05 μCi) and the respective inhibitors indicated in the figures at 37 °C for 5 min. After incubation, the astrocyte layer was thoroughly washed, trypsinized and glutamate uptake measured in aliquots with equal number of cells in triplicates as described for vesicular glutamate uptake in the previous section.

2.7. Immunohistochemistry

Mice were sacrificed under CO₂ anesthesia, perfused with 20 ml of 2.5% paraformaldehyde in PBS and postfixed brains equilibrated for 12 h at 4 °C in PBS containing 30% sucrose and 2 mM MgCl₂. Affinity purified polyclonal antibodies against the total *GLAST1* protein, monoclonal antibodies against GFAP (Boehringer Mannheim, G-3893) and Calbindin-D (C-8666) and alkaline phosphatase conjugated second antibodies were used for immunohistochemistry.

Apoptosis was analyzed by the *in situ* cell death detection kit (TUNNEL assay, TdT-mediated dUTP nick labeling (Boehringer Mannheim)).

2.8. Motor performance and behavioral testing

For behavioral testing mice of age 2–4 months were used. The Morris water maze test [38], the descending vertical pole, the horizontal bridge and inclined grid tests [53], the open field test [24], and the horizontal wire test [2] were performed following the established protocols.

2.8.1. Preparation of cerebellar slices

Sagittal sections (180 μ m) from the medial part of the mouse cerebellum from 8- to 14-day-old mice were prepared [26] and maintained at room temperature in carbogen (95% O₂, 5% CO₂) saturated, bicarbonate-buffered saline (in mM) 118 NaCl, 3 KCl, 1 MgCl₂, 25 NaHCO₃, 1 NaH₂PO₄, 1.5 CaCl₂, 20 glucose) at pH 7.4. Prior to recordings, slices were incubated for at least 1 h to allow recovery. If not indicated otherwise, 10- μ M bicuculline was added to bath solutions to block spontaneous synaptic activity. For whole cell recordings [20], slices were continuously superfused with the carbogen-saturated solution (10 ml/min) in the recording chamber under a Zeiss upright microscope.

2.8.2. Patch clamp recordings

In patch clamp experiments, Purkinje cells were selected by their intact overall shape, their ability to fire action potentials in drug-free solution, a high electrically input resistance and the occurrence of spontaneous synaptic activity. The intracellular pipette solution contained (in mM): 140 KCl, 10 HEPES, 2 MgCl₂, 2 ATP, 0.4 GTP, 10 EGTA, 1 CaCl₂ (adjusted to pH 7.2 with KOH). Borosilicate glass patch and stimulation pipettes were filled with intracellular solution, they had resistances of 1.5–3 M Ω . Voltage-clamp recordings were performed with a patch-clamp amplifier (EPC-7, HEKA ELEKTRONIK, Lambrecht, Germany). Input resistances of Purkinje cells varied around 1 G Ω . No series resistance compensation was made. Unless stated otherwise, whole cell currents were recorded with sampling frequencies of 5 kHz and filtered (3-pole-Bessel filter 10 kHz, 4-pole Bessel filter 2.9 kHz) before analysis.

2.8.3. Stimulation and application

Electrophysiological and stimulating signals were simultaneously recorded with EPC-7 hard- and software (Pulse Fit, HEKA, Germany). Afferent climbing- and parallel fibers were stimulated (HG.15, HI Med., England) recording Purkinje cell EPSCs. Impulses carried out at intervals of 2 s with 2–20 V.

NBQX (10–25 μ M), 10 μ M CPP and 10 μ M SYM2081, were added to bath solutions to block different glutamate receptors and transporters, respectively.

Calculations of EPSC-decay times and further analysis were performed off-line by using the software Pulsefit (HEKA, Germany) and IGOR (Wavemetrics, Oregon, USA).

Experiments were carried out in accordance with the guidelines of the Ethics Committee of the Medical Faculty at the Universities of Köln and Göttingen, Germany.

3. Results

3.1. Generation of the *GLAST1* mutant mouse line

A murine 6.3-kb genomic *GLAST1* clone harboring exons I and II was isolated from a mouse genomic leukocyte library, using the rat *GLAST1* cDNA as a probe [49] (Fig. 1A). The sequence of the exons corresponds to the genomic sequence of human *glast1* [48].

A 1.9-kb *NdeI/NdeI* fragment with exon II of the 6.3-kb insert was replaced by the neomycin resistance gene (*neo*) of the pPNT vector (Fig. 1A). Exon II codes for the translation start site, the intracellular N-terminal region and the first transmembrane domain of the *GLAST1* protein. Transfection by electroporation of CJ7 and R1 embryonic stem (ES) cells with the *ClaI* linearized replacement vector and negative/positive selection with G418 and gancyclovir yielded five positive ES cell clones. The homologous recombination event was verified by *NcoI* restriction and Southern blot hybridization analysis using the external 5' probe (Fig. 1B). ES cell clones were injected into CD1 blastocysts which led to two germline chimeric *glast1*^{+/-} male mice, which were used for breeding to homozygosity. The characterization of the *eaac1*^{-/-} mouse mutant has been extensively described [41]. Homozygous *glast1*^{-/-} and *eaac1*^{-/-} mice were crossbred to the homozygous *glast1*^{-/-}*eaac1*^{-/-} double mutant and characterized similarly. The diagnostic *NcoI* (10.8kb)- and *BamHI* (11 kb)-RFLPs [41] in Southern blot analysis of the *glast1* and *eaac1* loci, respectively, verified the genotypes, as described for the ES cells (Fig. 1B).

The substitution of the 1.9-kb *NdeI/NdeI* fragment with exon II by the *neo* cassette in littermates of F1 and F2 generation yielded *glast1* transcripts in Northern blot hybridization of brain RNA similar in size in homozygous and wt littermates. An exon II specific probe proved that exon II was deleted (Fig. 1C).

Solubilized proteins of partially enriched plasma membranes of brains of *wt*, *glast1*^{-/-} and *glast1*^{-/-}*eaac1*^{-/-} mice were separated on SDS-PAGE (12%) and probed in immunoblots with affinity purified rabbit anti-*GLAST1*, *EAAC1*- and *GLT1*-antibodies. Neither complete nor truncated immunoreactive *GLAST1* and *EAAC1* polypeptides were detected in the homozygous mice (Fig. 1D).

These results were confirmed by immunohistochemical analysis. The typical expression pattern of *GLAST1* in Bergmann glia arborising into the molecular layer of cerebellum in *wt* mice, which is absent in the cerebellum of *glast1*^{-/-} mice is displayed in Fig. 2A and B. The absence of *EAAC1* in the *eaac1*^{-/-} mutant has been

demonstrated earlier [41]. GLAST1 and EAAC1 antigens were absent in the double mutant mouse (not shown).

These results clearly demonstrated that we had generated the GLAST1- and the GLAST1/EAAC1 transporter deficient mouse lines.

3.2. Phenotypic characterization

The most surprising observation was the inconspicuous phenotype of *glast1*^{-/-} and *glast1*^{-/-}/*eaac1*^{-/-} littermates from birth to the age of 24 months with normal motor activity, gross behaviour and fertility, indistinguishable from *wt* progeny.

Similar to the EAAC1 deficiency [41], also *glast1*^{-/-} and *glast1*^{-/-}/*eaac1*^{-/-} mice do not compensate the loss of their respective glutamate neurotransmitter uptake

systems by upregulation on the transcriptional level of the other known L-glutamate transporters as estimated densitometrically in the Northern blot analysis (Fig. 1C). Densitometry of Western blot analysis of glutamate transporters GLT1 and of EAAT4 in equal protein aliquots of *wt* and *glast1*^{-/-} total brain protein extracts of 8-week-old male mice indicated that the concentration of the high affinity GLT1 gene translation product increases significantly (up to two to threefold) in the *glast1*^{-/-} mutant, whereas EAAT4 protein concentrations remained unaltered as documented in Fig. 2E. Glutamate uptake studies in primary astrocyte cultures from brains of the null allelic mice (Fig. 3A), as well as by membrane vesicles of *wt* and *glast1*^{-/-} brain and membrane vesicles of hemispheres and cerebellum (Fig. 3B and C), supported these findings.

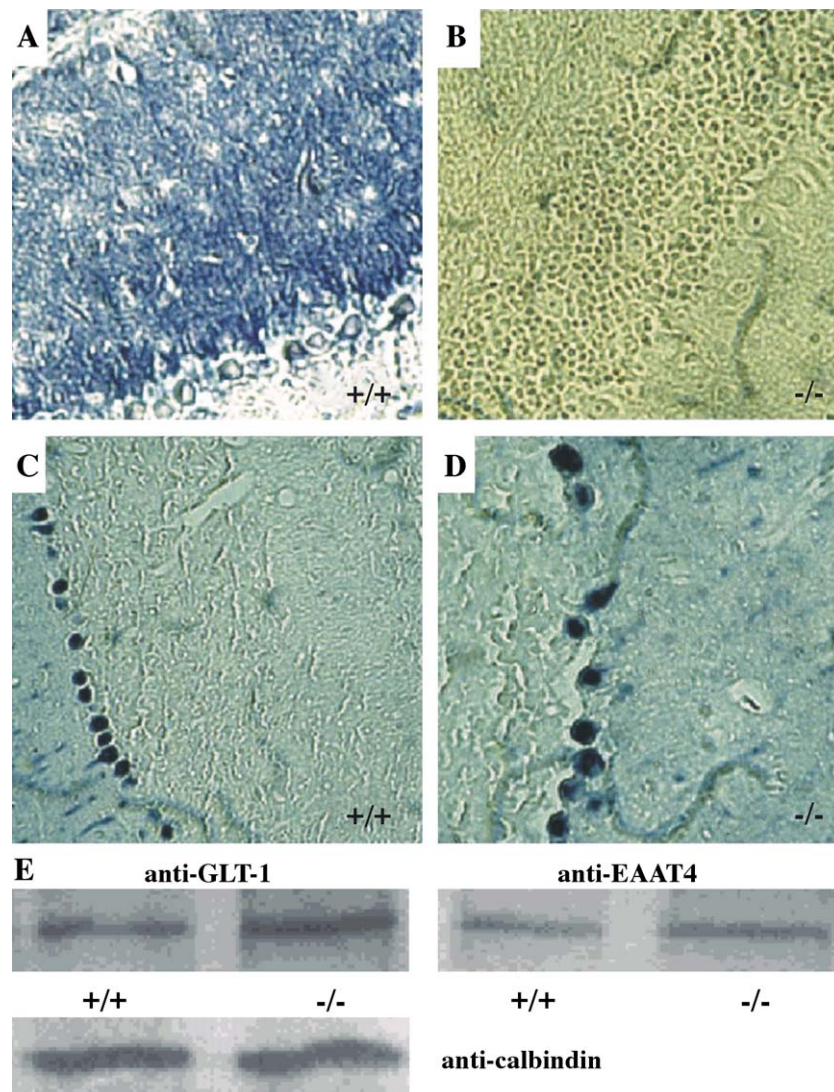


Fig. 2. Immunohistochemical analysis (A–D) and Western blot analysis (E). Cerebellar sections of *wt* and *glast1*^{-/-} mice, A and B stained with anti-GLAST1 antibody and alkaline phosphatase-conjugated second antibody, C and D with anti-Calbindin antibody. (E) Western blot of aliquots of total brain protein extracts of *wt* and *glast1*^{-/-} mice probed with anti GLT1, EAAT4 and calbindin antibodies. 20, 40 and 60 μ g of protein were used for PAGE separation, Western blotting and quantification using the SCION Image Quant software of the phosphoimager.

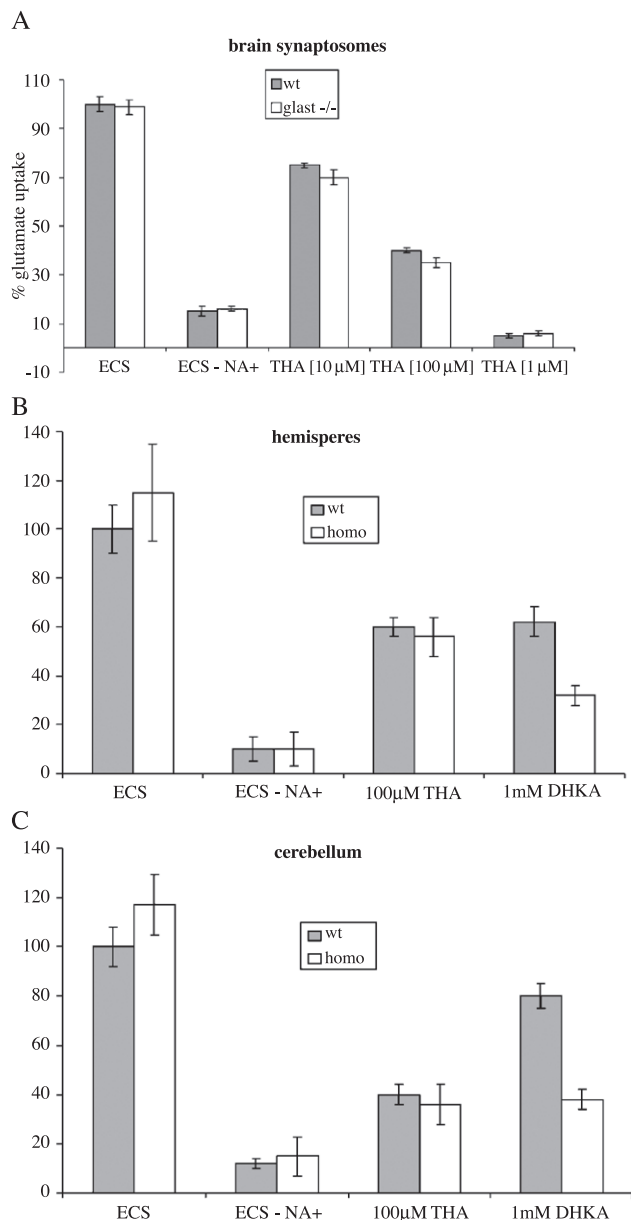


Fig. 3. Glutamate uptake in brain membrane vesicle preparations and astrocyte cultures of total brain of *wt* and *glast1*^{-/-} mice. (A) Glutamate uptake and THA inhibition. (B) [¹⁴C] L-Glutamate uptake by vesicle preparation of hemispheres and (C) of cerebellum of *wt* (+/+) and *glast1*^{-/-} (-/-) mice: Na⁺-dependent uptake, inhibition of neurotransmitter uptake by THA and dihydrokainate (DHKA).

3.3. Vesicular and astroglial glutamate uptake

Astroglia of the cortex and Bergmann glia cells in the granular cell layer of cerebellum strongly express GLAST1, GLT1 and EAAT4. We studied [¹⁴C] glutamate uptake and inhibition in vivo in primary cultures of astrocytes isolated from total brain of *wt* and *glast1*^{-/-} mice and in vitro in the well-established plasma membrane vesicle system [45]. These studies included the Na⁺ ion dependence of [¹⁴C] glutamate uptake and

transport inhibition in the presence of the two inhibitors L-threo-3 hydroxy-aspartate (THA) (Fig. 3A), and DHKA with cultured primary astrocytes isolated from total brain (Fig. 3B), and plasma membrane vesicles of hemispheres and cerebellum of *wt* and GLAST1 deficient mice, summarized in Fig. 3.

Glutamate uptake into vesicle preparations of the *wt* and *glast1*^{-/-} genotype was unperturbed, proved to be Na⁺-dependent, and threo D-hydroxyaspartate (THA) caused the well-known inhibition of glutamate transport comparable in *wt*, and the null mutants, 80%, 40% and 8% at 10, 100 and 1000 μM THA, respectively (Fig. 3A).

Control experiments confirmed the Na⁺ dependence of L-glutamate transport. Na⁺-free ECS reduced the transport on the average to 45% and 15% in astrocytes from total brain of *wt* and null mutants, respectively (Fig. 3A). THA (100 μM) concentration inhibited glutamate transport in plasma membrane vesicle preparation and astrocytes cultures of *wt* and *glast1*^{-/-} by 40% and 60% in vesicles of hemispheres and cerebellum, respectively (Fig. 3B and C).

Glutamate transport in the presence of GLT1-specific transporter dihydrokainate (DHKA) in vesicle preparations of hemispheres from *wt* brain was reduced by 40% and of cerebellum by 20% but in *glast1*^{-/-} hemisphere and cerebellum vesicle preparations were reduced by about 65% (Fig. 3B and C).

3.4. GLAST1 and EAAC1-deficiency and cerebellar structures

Purkinje cells (PCs) are the sole link between the cerebellar cortex and the cerebellar nuclei. This system might serve as a paradigm for the glutamatergic excitatory system. The morphology and number of Purkinje cells, the granular and molecular cell layers in cryosections of the cerebellum of 5-month-old *wt*, *glast1*^{-/-} and *glast1*^{-/-} *eaac1*^{-/-} mutant mice were indiscriminant in light microscopy (not shown).

High L-glutamate levels in the synaptic cleft leads to NMDA and AMPA receptors mediated opening of post-synaptic Ca²⁺ channels with Ca²⁺ influx which might induce the expression of the Ca²⁺ binding protein Calbindin-D in Purkinje cells. However immunohistochemically, the Calbindin D signal in Purkinje cells revealed no difference in the two mutants and *wt* mice (Fig. 2C–D).

Neurodegeneration is often followed by a reactive gliosis indicated by the upregulation of the expression of glial fibrillary acidic protein (GFAP) Immunostaining of cerebellar sections with the astrocyte-specific anti-GFAP antibody showed no gliosis in the molecular or granular cell layer of cerebellum of the mutant mice (data not shown).

In addition, no neuronal apoptosis due to glutamate neurotoxicity was observed when examined by the TUNNEL (TdT-mediated dUTP nick labeling) assay (data not shown).

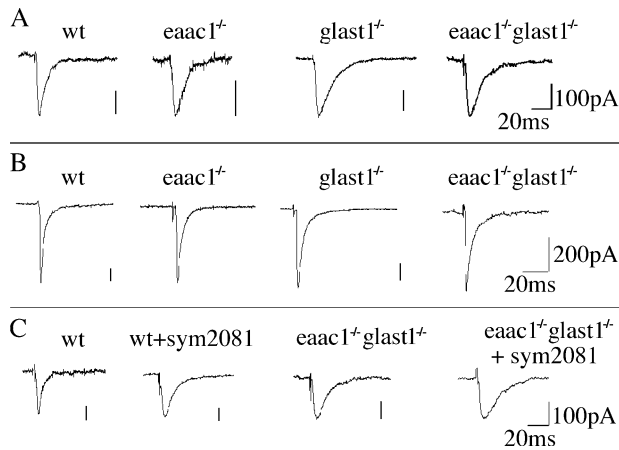


Fig. 4. Examples for recorded EPSCs at Purkinje cells after unitary stimulation of afferent parallel fibers (A) or climbing fibers (B) and (C) before and after adding the GLT-1 inhibitor SYM2081.

3.5. *GLAST1* deficient mice show normal spatial learning, cerebellar motor coordination and activity, and exploration

Locomotion, learning and memory of cohorts of 6-week-old *wt*, *glast1*^{-/-} and *eaac1*^{-/-} mice were examined in the Morris water maze task and their motor activity and exploration in the open field test. The motor coordination ability was challenged in the rotarod test. Neither task unmasked any motor deficits (data not shown).

3.6. Patch clamp recordings of EPSCs of Purkinje cells in cerebellar slices of *glast1*^{-/-}, *eaac1*^{-/-} and *glast1*^{-/-}*eaac1*^{-/-} mice

Functional parameters of glutamate receptor mediated excitatory postsynaptic currents (EPSCs) were analysed by patch clamp recordings on cerebellar Purkinje cells of 8–14-day-old mice in thin slice preparations [20,26] for the following reasons. First, Purkinje cells contain only rapidly deactivating AMPA receptor channels [5,29] assuring that the kinetic analysis of AMPA receptor mediated EPSCs (AMPA EPSCs) was not disturbed by a potential parallel activation of NMDA receptors. Second, Purkinje cells display extraordinary long-lasting AMPA EPSCs with a prolonged presence of glutamate in the synaptic cleft [5],

thus providing favourable conditions for the analysis of individual phenotypes with a disrupted glutamate transport. Third, selective activation of parallel and climbing fiber EPSCs allows to investigate synaptic responses under well-defined stimulation conditions. For patch clamp recordings, Purkinje cells were visualized using differential interference contrast optics [18,32]. After establishing the whole-cell recording configuration, spontaneous synaptic activity confirmed the good viability of the preparation (input resistance up to 1 GΩ and resting potential conditions around -65 mV).

To reliably isolate AMPA receptor mediated EPSCs from other synaptic responses, inhibitory GABA-receptor mediated currents were completely blocked by adding 10 μM bicuculline to extracellular solutions (ECS). The remaining spontaneous and stimulated synaptic responses were completely suppressed by adding 10 μM NBQX to ECS, identifying them as AMPA-mediated EPSCs. As expected, addition of 10 μM of the NMDA-channel blocker CPP to the bath solution showed no effect.

Whole-cell patch clamp recordings were performed in voltage clamp mode, with the stimulation pipette positioned above climbing- or parallel fibers. Electrical stimulation evoked robust EPSCs in Purkinje cells as previously reported [5]. For EPSC recordings, stimulus intensity was reduced to the minimum level where regular synaptic responses were still observed. In this case, stimulation of climbing fibers was associated with EPSC fluctuations according to the “all-or-nothing” rule, where parallel fibers responded proportional to stimulus intensity over a wide range of intensities [29].

Kinetic parameters of AMPA EPSCs in *wt*, *glast1*^{-/-}, *eaac1*^{-/-} and *glast1*^{-/-}*eaac1*^{-/-} were analysed during unitary stimulation of climbing or parallel fibers EPSCs. Under identical stimulation conditions, amplitudes of parallel and climbing fiber EPSCs were identical for *wt* and the three mutant lines (Fig. 4).

Previous reports have shown that blockade of glutamate transporters can significantly alter the recovery phase of EPSCs [5]. In *wt* mice, the average decay time constant of climbing fiber EPSCs was 3.5 ms. This was comparable to decay times of 4.1 ms found in *EAAC1*^{-/-}, but significantly faster than those found in *glast1*^{-/-} and *glast1*^{-/-}*eaac1*^{-/-}

Table 1

Kinetic parameters of EPSCs during stimulation at climbing and parallel fibers

(A) Decay time tau in ms±standard error of the mean				
	<i>wt</i>	<i>eaac1</i> ^{-/-}	<i>glast1</i> ^{-/-}	<i>glast1</i> ^{-/-} / <i>eaac1</i> ^{-/-}
Climbing fiber	3.5±0.2 (n=13)	4.1±0.1 (n=10)	5.0±0.9 (n=6)*	5.7±0.4 (n=12)*
Parallel fiber	5.9±0.3 (n=16)	6.2±0.4 (n=6)	8.0±0.6 (n=16)*	7.45±0.5 (n=12)*
(B) Rise times of parallel and climbing fiber EPSCs during unitary stimulation				
	<i>wt</i>	<i>eaac1</i> ^{-/-}	<i>glast1</i> ^{-/-}	Double ko
Climbing fiber	1.3±0.2 (n=13)	0.67±0.2 (n=10)	0.6±0.1 (n=6)	0.6±0.1 (n=5)
Parallel fiber	1.04±0.2 (n=11)	0.68±0.2 (n=6)	0.7±0.1 (n=20)	0.9±0.1 (n=10)

Rise times (10–90% max. ampl) in ms±standard error of the mean. Stars refer to significant differences between “knock out” and *wt*-values (*p*<0.05).

Table 2

Decay times of parallel fiber EPSCs during single and multiple stimulation (three stimuli separated by 20 ms)

	<i>wt</i>	<i>eaac1</i> ^{-/-}	<i>glast1</i> ^{-/-}	Double ko
Decay time (unitary stimul.)	5.9±0.3 (n=16)	6.2±0.4 (n=6)	8.0±0.6 (n=16)*	7.5±0.5 (n=12)*
Decay time (multiple stim.)	7.6±0.8 (n=13)	13.2±1.5 (n=8)*	21.8±2.4 (n=20)*	18.1±0.7 (n=10)*
Relative retardation	128.8%	212.9%	272.5%	241.3%

Decay time tau in ms±standard error of the mean. Stars refer to significant differences between “knock out” and *wt*-values (*p*<0.05).

mice with values of 5.0 and 5.7 ms, respectively. For parallel fiber stimulation, EPSCs displayed decay times of 5.9 ms in wild type animals, again similar to 6.2 ms found in

eaac1^{-/-} mice but significantly different from 8.0 and 7.5 ms found in *glast1*^{-/-} and *glast1*^{-/-}*eaac1*^{-/-} mice, respectively. No significant difference was found in rise times (10–90% max. amplitude) between *wt* and transgenic animals. For direct comparison, a summary of kinetic parameters is given in Table 1.

To assess the potential impact of EPSC amplitude on decay profiles, we performed an additional series of experiments based on multiple stimulation protocols. In this case, parallel fiber stimulation was performed by a series of three current pulses each separated by a time interval of 20 ms. As illustrated in Table 2, this stimulation was associated with a substantial prolongation of EPSCs in *wt* animals with a 129% retardation of decay time constants changing from 5.9 ms (unitary stimulation) to 7.6 ms (triple stimulation). EPSC decay time constants were significantly more affected in mutant animals, where relative changes were given by 213%, 273% and 241% for *eaac1*^{-/-}, *glast1*^{-/-} and *glast1*^{-/-}*eaac1*^{-/-}, respectively. These observations underline the important role of glutamate transporters EAAC1 and GLAST1 for clearance of glutamate from the synaptic cleft, in particular during strong stimulation of synaptic responses.

The double mutant further allowed the investigation of the potential role of additional glutamate transporters not directly affected by the mutations. Accordingly, we performed patch clamp recordings of EPSCs in the after bath application of SYM2081, a known blocker of glutamate transport [21]. In *wt* animals, decay time constants of parallel fiber EPSCs were prolonged from 5.9 to 14.3 ms, confirming the previously described role of glutamate transporters in shaping the profile of EPSCs (e.g. Ref. [5]). Interestingly, postsynaptic currents were similarly prolonged in *glast1*^{-/-}*eaac1*^{-/-} mice from 7.5 to 17.2 ms as illustrated in Fig. 5. This indicated that glutamate transport continued to be a prominent determinant of EPSC kinetics even when *glast1*^{-/-} and *eaac1*^{-/-} were knocked out by genetic manipulation.

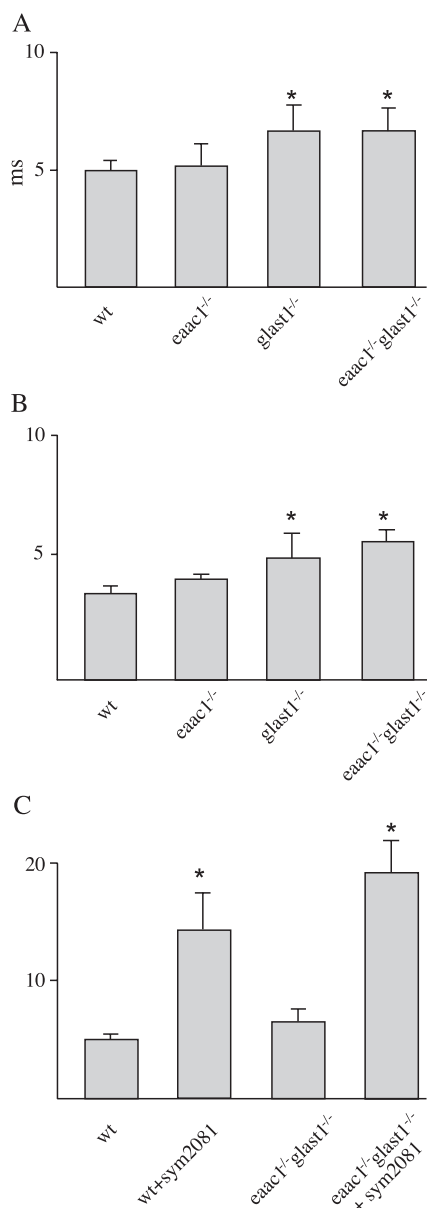


Fig. 5. Summary histograms showing the EPSC decay times at Purkinje cells after unitary stimulation of parallel fiber (A) and after climbing fiber stimulation (B) of *wt* mice and different knock-out mice. Panel C displays a summary of EPSC decay times of *wt* and *glast1*^{-/-}*eaac1*^{-/-} mice in the presence of the glutamate transporter inhibitor SYM2081. For details, see text.

4. Discussion

Here, we report a combined genetic and electrophysiological approach for the functional analysis of the main L-glutamate neurotransmitter transporters in two null-allelic mouse mutants deficient in the glial transporter GLAST1 (*glast1*^{-/-}) and in both GLAST1 and EAAC1 (*glast1*^{-/-}*eaac1*^{-/-}) in excitatory synapses of mouse CNS and

extended and exemplified electrophysiologically with cerebellar Purkinje cells of these genotypes.

In an earlier study, we described the *eaac1*^{-/-} mouse model [41]. EAAC1 is dominantly expressed in kidney and gut but weakly also in neurons of cerebellum and hippocampus. EAAC1 deficiency causes a massive hyperaminoaciduria but no neurotoxicity. Previous studies demonstrated the regional expression pattern of GLAST1 most prominently in Bergmann glia cells of cerebellum and less in the hippocampus and cortex [31,49], whereas GLT1 is expressed mainly in cortex, hippocampus and striatum and less so in cerebellum.

Glutamate is used as excitatory neurotransmitter in three pathways at terminals in the cerebellum: the climbing fibre input on Purkinje cell soma, the mossy fibre input into granular cells and the parallel fibres from granule cells to Purkinje dendrites [47]. Ca²⁺ entry through respective receptors due to high L-glutamate concentrations in the synaptic cleft may lead to a high Ca²⁺ influx into neurons [23], which is potentiated by entry through voltage-dependent calcium channels in axons of Purkinje cells [10]. An increased Calbindin-D expression specifically in Purkinje cells is thought to prohibit toxic intracellular Ca²⁺ concentrations [34]. In the single and double glutamate transporter deficient mutant mice, anti-Calbindin-D antibodies revealed no increased expression of the Ca²⁺ binding protein Calbindin-D, which might indicate that intracellular Ca²⁺ in Purkinje cells is not elevated in GLAST1 and EAAC1 deficient mice.

Neurotoxic and neurodegenerative disorders might lead to a reactive gliosis indicated by an upregulation of GFAP expression [3]. However, anti-GFAP antibodies disclosed no quantitative differences in GFAP expression in *glast1*^{-/-} mutant and *wt* mice.

We also probed the neuronal cell layers of the cerebellum and hippocampus of *glast1*^{-/-} mice for apoptosis using the TUNNEL assay (not shown). The histological and immunohistochemical results clearly exclude cell degeneration or apoptosis in the mutant mouse lines described here.

Cerebellar L-glutamatergic synapses influence motor coordination [1]. Mice lacking glutamate receptors GluR1 and GluR2 [16] develop a severe cerebellar atactic gait and intention tremor. Surprisingly, homozygous *glast1*^{-/-} and the *glast1*^{-/-}*eaac1*^{-/-} double mutant mice had a coordinated gait and responded like *wt* mice when challenged in tasks which probed for challenged motor coordination, motor activity, learning and memory. The *glast1*^{-/-} mouse mutant has been generated earlier with a different gene targeting construct [54]. This mutant differed from our *glast1*^{-/-} mutant and the *glast1*^{-/-}/*eaac1*^{-/-} double mutant in motor coordination only at a high-speed rotarod challenge (>20 vs. 10 rpm in our experiments). This might express a strain difference.

In a recent study [46], antisense oligonucleotides of the three main glutamate transporters GLAST1, GLT-1 and EAAC1 were administered intrathecally to mice to mimic

respective “knock outs”. A reduced expression of the transporters was observed. GLAST1 and GLT-1 antisense oligonucleotides caused neurodegeneration and progressive paralysis whereas EAAC1 deficiency resulted in mild neurotoxicity. Here, we applied the genetic approach to unravel the function (s) of the individual glutamate transporters via the conventional “knock out” models which unveiled the surprising phenotypes described above and which are at variance with the reported observations. The conflicting results might be caused by the different experimental strategies, null allelic mutation versus intracerebral antisense oligonucleotide application.

Different from the *glast1*^{-/-} and the *glast1*^{-/-}*eaac1*^{-/-} mice described here and the *eaac1*^{-/-} mutant described previously [41], the recently described GLT-1-deficient mouse [51] developed severe neurological symptoms such as epilepsy leading to early death. The replacement vector used for the “knock out” of *glt-1*, however, could allow the synthesis of a truncated, hydrophobic N-terminus of GLT-1. Cytotoxic effects of putative derived peptides, which are not detected by the antibodies used in this study, remain to be excluded. GLAST1 deficiency might induce the upregulation of the other L-glutamate transporters, particularly of GLT-1, which colocalizes with GLAST1 in several regions of CNS (cerebellum, hippocampus) and EAAT-4, also highly expressed in Purkinje cells [55]. This raised the question whether these transporters, remaining intact in the single and double null allelic mutants, compensate for the deficient transport function of GLAST1 of Bergmann glia cells. Quantitative RT-PCR and Northern blot analysis did not reveal an upregulation of the other high affinity glutamate transporters on the transcriptional level, although repeated Western blot analysis of GLT1 in protein aliquots of the respective total brain extract indicated an about twofold GLT1 concentration over *wt* (Fig. 2E). This observation does not exclude an additional activation of the GLT1 activity, as e.g. protein phosphorylation of GLT1 [11,12] and for EAAC1 [19], which remains to be studied.

The activity of the glutamate transporters discovered so far are supposed to be sufficient for an effective glutamate reuptake from CNS glutamatergic synapses [45].

The phenotype with the missing neuropathological and behavioral symptoms and the biochemical analytical results of the GLAST1 and GLAST1/EAAC1 deficient mutant mice were unexpected except the hyperamino aciduria of the double mutant contributed by the mutated *eaac1* locus suggested a compensatory of the redundant glutamate transporter systems. We therefore carried out additional functional analyses of the different transporters in these well-defined mouse mutants which included uptake studies of the labeled neurotransmitter glutamate and electrophysiological techniques.

Vesicle (synaptosomal) preparations and primary astrocytes from *wt* and *glast1*^{-/-} mouse brains showed no significant differences in glutamate uptake between the two

genotypes with small standard deviations below 8–10% after subtraction of the Na⁺-free transport.

Glu transport in the GLAST1 deficient and the double mutant is inhibited concentration dependent by L-threo-3-hydroxyaspartat, at a concentration of 100 μM THA the transport was reduced to 26% and 24% in wt and *glast1*^{-/-}, respectively. Among the few inhibitors of high affinity Na⁺-dependent glutamate transport systems dihydrokainate is known as a weak inhibitor [52], which has no effect on GLAST1 [27,28], however on GLT1 [42]. The inhibitory effect of DHKA on glutamate transport by primary astrocytes from wt mice in culture even of the high 1 mM concentration, is very weak (Fig. 3A), but in the GLAST1 deficient mutant by about 40%. Detailed quantitative and immunocytochemical studies on the differential expression of GLAST1 and GLT1 in rat brain revealed, that both transporters are roughly equally distributed throughout the hemispheres and brainstem, GLAST1 preferentially in the molecular layer of cerebellum and GLT1 in astrocytes of the hippocampus, cortex and striatum. GLAST1 and GLT1 transporter proteins are concomitantly expressed, though in different ratios in different regions of the brain [31]. In view of the complexity of the distribution, the simultaneous expression in the same cell with the possibility to form heterodimers or multimers with a broad functional diversity and the presence of GLT1 mRNA, e.g. in CA3 hippocampal neurons but the lack of protein in these cells, which suggests a posttranscriptional regulation, quantitative conclusions from inhibition experiments in a whole population of astrocytes isolated from total brain can only be made with precaution. Yet together with the membrane vesicle uptake and inhibition experiments (Fig. 3B and C), they suggest a compensatory function of GLT1 in brain regions with simultaneous expression of GLAST1 and GLT1 of the mutants.

A unique opportunity to evaluate the contribution of glutamate transport to synaptic neurotransmitter profiles comes from the electrophysiological analysis of Purkinje cell EPSCs in wt and mutant animals. For several reasons, cerebellar Purkinje cells provided the most attractive model system for this analysis. First, previous studies have established Purkinje cells as one of the best-characterized neuronal systems to study neurotransmitter profiles in the synaptic [5]. Second, the prolonged time course of neurotransmitter concentrations in Purkinje cell synapses provides extraordinary favourable conditions for the detection of subtle changes in the profile of synaptic glutamate transport. In parallel and climbing fiber synapses, one of our most significant results was the retardation of EPSCs after knockout of GLAST1, while genetic disruption of EAAC1 was associated with no detectable EPSC prolongation. Both observations are in agreement with a model where GLAST1 displays a modulatory effect on synaptic glutamate transients, while EAAC1 is primarily involved in regulating basal glutamate levels outside the synaptic cleft. These observations were different from those obtained under

multiple stimulation conditions, where both knock-out of EAAC1 and GLAST1 were associated with significant prolongations of EPSC decay times.

Our results obtained on *glast1*^{-/-} and *glast1*^{-/-}*eaac1*^{-/-} mice were well compatible with those previously reported on mouse models of glutamate transporter knock-out animals under different stimulation and recording conditions [33,54]. For example, our observation of prolonged EPSC decay times correlates with the previously noted prolongation of parallel fiber EPSCs in GLAST1 knock-out Purkinje cells [33]. Moreover, the increasing functional importance of GLAST1 and EAAC1 during multiple stimulation presented in this report is paralleled by observations of Marcaggi et al., who reported substantial prolongations of EPSC decays during high-intensity stimulation in their model system of *glast1*^{-/-}.

In summary, the glutamate transporter mutants described in this report will allow the analysis of the function of the individual transporters in the profiling of other excitatory synapses throughout the brain. The gene targeting strategy by conditional gene ablation (cell and developmental stage specific) might unravel the contribution of potential adaptive processes during development of the conventional glutamate transporter “knock out” models.

Acknowledgement

The support by the Deutsche Forschungsgemeinschaft and the Center of Molecular Medicine Cologne (CMMC) is gratefully acknowledged.

References

- [1] A. Aiba, M. Kano, C. Chen, M.E. Stanton, G.D. Fox, K. Herrup, T.A. Zwingman, S. Tonegawa, Deficient cerebellar long-term depression and impaired motor learning in mGluR1 mutant mice, *Cell* 79 (1994) 377–388.
- [2] J. Altmann, Observational study of behavior: sampling methods, *Behaviour* 49 (1974) 227–267.
- [3] J.A. Amat, H. Ishiguro, K. Nakamura, W.T. Norton, Phenotypic diversity and kinetics of proliferating microglia and astrocytes following cortical stab wounds, *Glia* 16 (1996) 368–382.
- [4] J.L. Arriza, S. Eliasof, M.P. Kavanaugh, S.G. Amara, Excitatory amino acid transporter 5, a retinal glutamate transporter coupled to a chloride conductance, *Proc. Natl. Acad. Sci. U. S. A.* 94 (1997) 4155–4160.
- [5] B. Barbour, B.U. Keller, I. Llano, A. Marty, Prolonged presence of glutamate during excitatory synaptic transmission to cerebellar Purkinje cells, *Neuron* 12 (1994) 1331–1343.
- [6] M.F. Bear, R.C. Malenka, Synaptic plasticity: LTP and LTD, *Curr. Opin. Neurobiol.* 4 (1994) 389–399.
- [7] G. Bensimon, L. Lacomblez, V. Meininger, A controlled trial of riluzole in amyotrophic lateral sclerosis. ALS/Riluzole Study Group, *N. Engl. J. Med.* 330 (1994) 585–591.
- [8] T.V. Bliss, G.L. Collingridge, A synaptic model of memory: long-term potentiation in the hippocampus, *Nature* 361 (1993) 31–39.
- [9] A. Bradley, *Production and Analysis of Chimeric Mice*, IRL Press, Oxford, 1987, pp. 113–151.

- [10] G. Callewaert, J. Eilers, A. Konnerth, Axonal calcium entry during fast 'sodium' action potentials in rat cerebellar Purkinje neurones, *J. Physiol. (Lond.)* 495 (1996) 641–647.
- [11] M. Casado, F. Zafra, C. Aragon, C. Gimenez, Activation of high-affinity uptake of glutamate by phorbol esters in primary glial cell cultures, *J. Neurochem.* 57 (1991) 1185–1190.
- [12] M. Casado, A. Bendahan, F. Zafra, N.C. Danbolt, C. Aragon, C. Gimenez, B.I. Kanner, Phosphorylation and modulation of brain glutamate transporters by protein kinase C, *J. Biol. Chem.* 268 (1993) 27313–27317.
- [13] D.W. Choi, Ionic dependence of glutamate neurotoxicity, *J. Neurosci.* 7 (1987) 369–379.
- [14] D.W. Choi, Glutamate neurotoxicity and diseases of the nervous system, *Neuron* 1 (1988) 623–634.
- [15] P. Chomczynski, N. Sacchi, Single-step method of RNA isolation by acid guanidinium thiocyanate–phenol–chloroform extraction, *Anal. Biochem.* 162 (1987) 156–159.
- [16] F. Conquet, Z.I. Bashir, C.H. Davies, H. Daniel, F. Ferraguti, F. Bordi, K. Franz-Bacon, A. Reggiani, V. Matarese, F. Conde, et al., Motor deficit and impairment of synaptic plasticity in mice lacking mGluR1, *Nature* 372 (1994) 237–243.
- [17] Y. Dehnes, F.A. Chaudhry, K. Ullensvang, K.P. Lehre, J. Storm-Mathisen, N.C. Danbolt, The glutamate transporter EAAT4 in rat cerebellar Purkinje cells: a glutamate-gated chloride channel concentrated near the synapse in parts of the dendritic membrane facing astroglia, *J. Neurosci.* 18 (1998) 3606–3619.
- [18] H.U. Dodt, W. Ziegler, Visualization of neuronal form and function in brain slices by infrared videomicroscopy, *Histochem. J.* 30 (1998) 141–152.
- [19] L.A. Dowd, M.B. Robinson, Rapid stimulation of EAAC1-mediated Na⁺-dependent L-glutamate transport activity in C6 glioma cells by phorbol ester, *J. Neurochem.* 67 (1996) 508–516.
- [20] F.A. Edwards, A. Konnerth, B. Sakmann, T. Takahashi, A thin slice preparation for patch clamp recordings from neurones of the mammalian central nervous system, *Pflügers Arch.* 414 (1989) 600–612.
- [21] S. Eliasof, H.B. McIlvain, R.E. Petroski, A.C. Foster, J. Dunlop, Pharmacological characterization of threo-3-methylglutamic acid with excitatory amino acid transporters in native and recombinant systems, *J. Neurochem.* 77 (2001) 550–557.
- [22] W.A. Fairman, R.J. Vandenberg, J.L. Arriza, M.P. Kavanaugh, S.G. Amara, An excitatory amino-acid transporter with properties of a ligand-gated chloride channel, *Nature* 375 (1995) 599–603.
- [23] M.P. Goldberg, D.W. Choi, Combined oxygen and glucose deprivation in cortical cell culture: calcium-dependent and calcium-independent mechanisms of neuronal injury, *J. Neurosci.* 13 (1993) 3510–3524.
- [24] C.S. Hall, *J. Comp. Physiol. Psychol.* 18 (1934) 385–403.
- [25] Y. Kanai, M. Stelzner, S. Nussberger, S. Khawaja, S.C. Hebert, C.P. Smith, M.A. Hediger, The neuronal and epithelial human high affinity glutamate transporter. Insights into structure and mechanism of transport, *J. Biol. Chem.* 269 (1994) 20599–20606.
- [26] B.U. Keller, A. Konnerth, Y. Yaari, Patch clamp analysis of excitatory synaptic currents in granule cells of rat hippocampus, *J. Physiol.* 435 (1991) 275–293.
- [27] U. Klockner, T. Storck, M. Conradt, W. Stoffel, Electrogenic L-glutamate uptake in *Xenopus laevis* oocytes expressing a cloned rat brain L-glutamate/L-aspartate transporter (GLAST-1), *J. Biol. Chem.* 268 (1993) 14594–14596.
- [28] U. Klockner, T. Storck, M. Conradt, W. Stoffel, Functional properties and substrate specificity of the cloned L-glutamate/L-aspartate transporter GLAST-1 from rat brain expressed in *Xenopus* oocytes, *J. Neurosci.* 14 (1994) 5759–5765.
- [29] A. Konnerth, J. Dreessen, G.J. Augustine, Brief dendritic calcium signals initiate long-lasting synaptic depression in cerebellar Purkinje cells, *Proc. Natl. Acad. Sci. U. S. A.* 89 (1992) 7051–7055.
- [30] K.P. Lehre, L.M. Levy, O.P. Ottersen, J. Storm-Mathisen, N.C. Danbolt, Differential expression of two glial glutamate transporters in the rat brain: quantitative and immunocytochemical observations, *J. Neurosci.* 15 (1995) 1835–1853.
- [31] K.P. Lehre, S. Davanger, N.C. Danbolt, Localization of the glutamate transporter protein GLAST in rat retina, *Brain Res.* 744 (1997) 129–137.
- [32] I. Llano, J. Dreessen, M. Kano, A. Konnerth, Intradendritic release of calcium induced by glutamate in cerebellar Purkinje cells, *Neuron* 7 (1991) 553–577.
- [33] P. Marcaggi, D. Billups, D. Attwell, The role of glial glutamate transporters in maintaining the independent operation of juvenile mouse cerebellar parallel fibre synapses, *J. Physiol.* 552 (2003) 89–107 (Epub 2003 Jul 23).
- [34] M.P. Mattson, B. Rychlik, C. Chu, S. Christakos, Evidence for calcium-reducing and excitoprotective roles for the calcium-binding protein calbindin-D28k in cultured hippocampal neurons, *Neuron* 6 (1991) 41–51.
- [35] M.L. Mayer, G.L. Westbrook, The physiology of excitatory amino acids in the vertebrate central nervous system, *Prog. Neurobiol.* 28 (1987) 197–276.
- [36] K.D. McCarthy, J. de Vellis, Preparation of separate astroglial and oligodendroglial cell cultures from rat cerebral tissue, *J. Cell Biol.* 85 (1980) 890–902.
- [37] D.T. Monaghan, R.J. Bridges, C.W. Cotman, The excitatory amino acid receptors: their classes, pharmacology, and distinct properties in the function of the central nervous system, *Annu. Rev. Pharmacol. Toxicol.* 29 (1989) 365–402.
- [38] R.G. Morris, P. Garrud, J.N. Rawlins, O.K. J. Place navigation impaired in rats with hippocampal lesions, *Nature* 297 (1982) 681–683.
- [39] Y. Mukainaka, K. Tanaka, T. Hagiwara, K. Wada, Molecular cloning of two glutamate transporter subtypes from mouse brain, *Biochim. Biophys. Acta* 1244 (1995) 233–237.
- [40] J.W. Olney, T. de Gubareff, Glutamate neurotoxicity and Huntington's chorea, *Nature* 271 (1978) 557–559.
- [41] P. Peghini, J. Janzen, W. Stoffel, Glutamate transporter EAAC1-deficient mice develop dicarboxylic aminoaciduria and behavioral abnormalities but no neurodegeneration, *EMBO J.* 16 (1997) 3822–3832.
- [42] G. Pines, N.C. Danbolt, M. Bjoras, Y. Zhang, A. Bendahan, L. Eide, H. Koepsell, J. Storm-Mathisen, E. Seeberg, B.I. Kanner, Cloning and expression of a rat brain L-glutamate transporter (published erratum appears in *Nature* 360 (1992 Dec 24–31) (6406) 768). *Nature* 360 (1992) 464–467.
- [43] A. Plaitakis, J.T. Carosco, Abnormal glutamate metabolism in amyotrophic lateral sclerosis, *Ann. Neurol.* 22 (1987) 575–579.
- [44] A. Plaitakis, E. Constantakakis, J. Smith, The neuroexcitotoxic amino acids glutamate and aspartate are altered in the spinal cord and brain in amyotrophic lateral sclerosis, *Ann. Neurol.* 24 (1988) 446–449.
- [45] J.D. Rothstein, L.J. Martin, R.W. Kuncl, Decreased glutamate transport by the brain and spinal cord in amyotrophic lateral sclerosis, *N. Engl. J. Med.* 326 (1992) 1464–1468.
- [46] J.D. Rothstein, M. Dykes-Hoberg, C.A. Pardo, L.A. Bristol, L. Jin, R.W. Kuncl, Y. Kanai, M.A. Hediger, Y. Wang, J.P. Schielke, D.F. Wely, Knockout of glutamate transporters reveals a major role for astroglial transport in excitotoxicity and clearance of glutamate, *Neuron* 16 (1996) 675–686.
- [47] P. Somogyi, K. Halasy, J. Somogyi, J. Storm-Mathisen, O.P. Ottersen, Quantification of immunogold labelling reveals enrichment of glutamate in mossy and parallel fibre terminals in cat cerebellum, *Neuroscience* 19 (1986) 1045–1050.
- [48] W. Stoffel, J. Sasse, M. Duker, R. Muller, K. Hofmann, T. Fink, P. Lichter, Human high affinity, Na⁽⁺⁾-dependent L-glutamate/L-aspartate transporter GLAST-1 (EAAT-1): gene structure and localization to chromosome 5p11-p12, *FEBS Lett.* 386 (1996) 189–193.

- [49] T. Storck, S. Schulte, K. Hofmann, W. Stoffel, Structure, expression, and functional analysis of a Na(+)-dependent glutamate/aspartate transporter from rat brain, *Proc. Natl. Acad. Sci. U. S. A.* 89 (1992) 10955–10959.
- [50] M. Szatkowski, D. Attwell, Triggering and execution of neuronal death in brain ischaemia: two phases of glutamate release by different mechanisms, *Trends Neurosci.* 17 (1994) 359–365.
- [51] K. Tanaka, K. Watase, T. Manabe, K. Yamada, M. Watanabe, K. Takahashi, H. Iwama, T. Nishikawa, N. Ichihara, T. Kikuchi, et al., Epilepsy and exacerbation of brain injury in mice lacking the glutamate transporter GLT-1, *Science* 276 (1997) 1699–1702.
- [52] P.C. Waldmeier, P. Wicki, J.J. Feldtrauer, Release of endogenous glutamate from rat cortical slices in presence of the glutamate uptake inhibitor *L-trans*-pyrrolidine-2,4-dicarboxylic acid, *Naunyn-Schmiedeberg's Arch. Pharmacol.* 348 (1993) 478–485.
- [53] J.E. Wallace, E.E. Krauter, B.A. Campbell, Motor and reflexive behaviour in the aging rat, *J. Gerontol.* 35 (1980) 364–370.
- [54] K. Watase, K. Hashimoto, M. Kano, K. Yamada, M. Watanabe, Y. Inoue, S. Okuyama, T. Sakagawa, S. Ogawa, N. Kawashima, et al., Motor discoordination and increased susceptibility to cerebellar injury in GLAST mutant mice, *Eur. J. Neurosci.* 10 (1998) 976–988.
- [55] K. Yamada, M. Watanabe, T. Shibata, K. Tanaka, K. Wada, Y. Inoue, EAAT4 is a post-synaptic glutamate transporter at Purkinje cell synapses, *NeuroReport* 7 (1996) 2013–2017.